VALIDITY OF TESTING SMALL ASPHALT CONCRETE MIXTURE BEAMS IN THE BENDING BEAM RHEOMETER

by

Crystal Rae Clendennen-Peirce

A thesis submitted to the faculty of
The University of Utah
in partial fulfillment of the requirements of the degree of

Master of Science

Department of Civil and Environmental Engineering

The University of Utah

December 2013

The University of Utah Graduate School

STATEMENT OF THESIS APPROVAL

The thesis of Crystal Rae Clendennen-Peirce

has been approved by the following supervisory committee members:

Pedro Romero	, Chair	October 11, 2013 Date Approved
Amanda Bordelon	, Member	October 11, 2013 Date Approved
Michael Barber	, Member	October 14, 2013 Date Approved

and by Michael Barber , Chair of

the Department of Civil and Environmental Engineering

and by David B. Kieda, Dean of The Graduate School.

ABSTRACT

This work uses three asphalt concrete mixtures with decreasing nominal maximum aggregate size (NMAS) to evaluate the validity of using the bending beam rheometer (BBR) to obtain flexural creep modulus of asphalt concrete mixture beams. The flexural creep modulus of asphalt pavement is an important property used to give insight into the cold property behaviors of the pavement. Previous research has indicated that asphalt mixtures can be tested using small beam samples (12.7-mm x 6.35-mm x 127-mm) in the BBR. Given that some of the dimensions are smaller than the aggregate used in the mixture, there is a concern that significant errors would be introduced due to the influence of these larger aggregate, thus the test is not being conducted on the representative volume element (RVE). This paper evaluates this concern. To accomplish this, three mix designs with NMAS, 12.5-mm, 9.5-mm, and 4.75-mm were developed and tested in the BBR. The 12.5-mm NMAS mixture was an actual mix placed on SR-201 in Salt Lake City; the 9.5-mm and 4.75-mm NMAS mixtures were developed to decrease the ratios of NMAS to beam width and NMAS to beam thickness. This approach is meant to imitate the development of an RVE while maintaining the beam size of 12.7-mm width x 6.35-mm thickness x 127-mm length. The two smaller mixtures were developed to be scaled equivalents of the 12.5-mm NMAS with similar volumetric parameters and gradation shapes. A series of experiments using the BBR were performed to calculate the creep modulus of the asphalt mixture beams. Through statistical analysis

it was found that flexural creep modulus data obtained from the BBR testing come from a normal distribution with equal variances across different sample groups. This means that the large aggregate mixtures resulted in no more variability than the smaller aggregate mixtures. Consequently, creep modulus data from asphalt mixture beams collected using the BBR could be used to predict the thermal properties of asphalt mixtures. Thus, based on these results, it is concluded that the small beam samples can be tested in the BBR as they meet the minimum RVE requirements.

TABLE OF CONTENTS

LIST OF FIGURES

LIST OF TABLES

OBJECTIVE

The objective of this work is to determine if the bending beam rheometer (BBR) can be used to get fast, reliable, flexural creep modulus information about small asphalt mixture beams.

BACKGROUND

In freeze areas of the US and Canada many notice the premature deterioration of asphalt pavements during the cold months. This is due to improper design of the asphalt mixture to withstand these changes in temperature. The road surfaces crack leading to water intrusion and accelerated damage. Highway agencies spend billions of dollars on maintenance and repair of pavement structures due to this accelerated damage [1]. Many highway agencies are striving to find an effective way to maximize the service life and facilitate improvements of low temperature performance in asphalt concrete pavements. Performance testing of asphalt concrete mixtures is one way to address this issue.

There are many tests that have been developed to determine the cold properties of asphalt concrete mixtures. For many years the most common test may have been the indirect tensile test (IDT) [2]. The IDT determines the creep compliance of asphalt concrete mixtures and uses visco-elastic principles to predict the stresses caused by thermal gradients [3]. Through years of use and research the IDT has been greatly improved and standardized to ensure meaningful results. Standardized protocols have been integrated to predict the actual asphalt pavement performance from IDT results [4]-[6]. Two other tests that have also been developed to evaluate low temperature asphalt pavement properties are thermal stress restraint specimen test (TSRST) [7]-[9], and the disc-shaped compact tension (DC(T)) Test [10]-[13]. Many researchers have investigated the applicability of these tests; and while these tests have many positive features none of

them has gained global popularity. Aside from research projects, none of these tests have been adopted for regular mixture testing for either design or control of the low temperature properties of asphalt mixtures. In fact, as of this writing, no highway agency has adopted any mixture test to control the quality of asphalt mixtures based on their potential for thermal induced cracking. Some reasons that a standard low temperature test has not been adopted include the amount of material needed, the cost and size of the testing equipment and refrigeration units, the complexity of data analysis or interpretation, the training of laboratory staff, and possibly others.

In 2005 Zofka and Marasteanu [14]-[17] and again in 2009 Ho and Romero [18] proposed a simple, fast, relatively inexpensive, and highly repeatable method of testing small beam specimen (12.7-mm x 6.35-mm x 127-mm) using the bending beam rheometer BBR, customarily used for performance grading (PG) of asphalt binders. Through this research the creep compliance of the asphalt mixture can be used to control low temperature properties in a way comparable with the IDT. Ho and Romero also showed that these results can easily be used to predict thermal stresses during field construction [19], [20].

Both the IDT and the BBR record the time-dependent tensile response of the material due to a creep load at a specific temperature. However, comparisons of the same material have shown some differences in results between these two test methods [21]. These differences are believed to be the result of differences in gauge length and or differences in stress state. The effective gauge length used in BBR testing is the distance between supports, 104 mm, while the IDT, as developed during the Strategic Highway Research Program (SHRP), records deformation over a 25 mm gauge length. The stress

state between those two test are different; in the BBR the measurement is done in bending (with tension on the bottom of the beam) while in the IDT there is compression in the vertical axis inducing tension on the horizontal axis. These tests do not necessarily result in the same numbers for creep compliance but, comparisons between the two of them are highly correlated [20]. More research is needed if these differences are to be resolved.

Many studies have demonstrated that small asphalt mixture samples can be used to obtain mechanical properties and predict mixture behavior [19]. Still, this approach of testing small asphalt concrete beams is met with skepticism. Critics are concerned with the beam size in relation to the maximum aggregate size. These critics are hesitant to accept that these small samples are in fact the representative volume elements (RVE) of the material. Velásquez et al. conducted a study to determine the effect of beam size on the creep modulus of asphalt mixtures at high, intermediate, and low temperatures [21]. In that work the beam sizes were increased to see if the size of the beams had an effect on the creep compliance. For the smallest size, the BBR was used; but for the subsequent larger sizes equipment designed for the purpose of the research was designed. Velásquez concluded that the creep compliance was affected by the beam size at high and low temperatures. Although, Velásquez also concluded that the cold temperature fluctuation could be due to ice build up on the measurement devices and the beams themselves. This rationalizes concerns of not only beam size to maximum aggregate size ratio, but also the call for proper equipment and standardization of testing.

This work addresses the concern of small beam size to aggregate size ratio through a different approach. In this work three equivalent mixtures with decreasing

nominal maximum aggregate sizes (NMAS) were analyzed. The three different mixtures were evaluated to ensure that the mixtures were in fact equivalent by comparing the volumetric parameters and the gradations. An alternative validation was done by visually analyzing scanned images of the three mixes at the optimum asphalt content. The BBR measurements were collected from the three groups and the variances of the data groups were proven to be equal using Bartlett's test. Bartlett's test relies on the data being normally distributed and tests based on empirical distribution function (EDF) statistic confirmed this.

REPRESENTATIVE VOLUME ELEMENT

The representative volume element or RVE is a certain volume of the composite material that has been determined through calculation and laboratory testing to represent the global properties of the material. Traditionally an RVE is selected by starting with a sample whose smallest dimension is of nominal maximum aggregate size (NMAS); the samples are tested and the sample size is increased accordingly to obtain a normalized variability. The intent of determining if the RVE is met, is to ensure that all individual materials of a composite are present for testing. For example, if we have a composite material consisting of aggregate, air, and binder, we want an RVE that contains all three components in enough quantities so that when tested, the response is dependant on all components. Take the two-dimensional example of the X-ray tomography image in Figure 1: When the representative area element (RAE) is very small the % Aggregate can vary from 0% to 100%. As the area is increased the fluctuations in % Aggregate abate and when the fluctuations stabilize this area is the RAE of the sample.

It would be meaningless to have an RAE or RVE that has only binder and air, or binder and aggregate when there are three components to the composite. Having a volume that is not representative of the whole composite material would results in extreme fluctuations in variability of results obtained through any testing. A sample volume consisting of only air and binder would result in a very different creep modulus, for example, than a volume consisting of only binder and aggregate. If the variability of

measured results from sample to sample is stable then the minimum requirement of the RVE has been met.

Composite theory states that in composite materials having spatial disorder with no microstructural periodicity (asphalt concrete mixtures) the determination of any stress, strain, or energy field can be measured as an average over the given domain [23]-[24]. Therefore the stress or strain recorded as part of any analysis is not the actual value experienced by a specific component but rather an average or bulk property over the given section. The question asked then is whether this averaging is done over the entire domain that includes all heterogeneities or whether it is influenced by localized phenomenon. This answer depends on the property being measured and the shape of the sample. The size of the domain that satisfies these averaging requirements is the RVE [25].

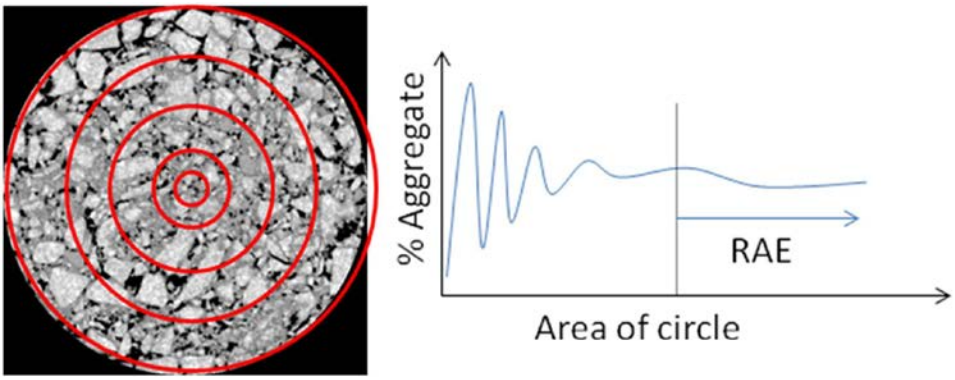

Figure 1: X-Ray Tomography Image for RVE Conceptualization [22]

APPROACH

It is customary in determining the RVE to increase the size of the analyzed volume until a statistical stability is reached. As an example, consider a chain with three randomized components: a large steel link, a medium copper link, and a small iron link as shown in Figure 2. Consider the case where a small sample of this composite material is tested in the laboratory for its elongation, as shown in Figure 3. Depending on the location of the sample size, the percent steel in the sample can vary between 0% (no steel) and 100% (all steel). The resulting measured elongation of this sample might result in large fluctuations depending on whether some lengths contain steel while others do not. This sample length does not represent all elements of the chain; the length in Figure 3 is not the RVE of this composite material. However, as the sample length is increased, the fluctuations in measured elongation due to variations in steel content greatly abate. In this case, the length at which the elongation function stabilizes is the minimum size needed to overcome the domain of small scale heterogeneity. This domain is the RVE. In general, the RVE ensures a given accuracy of the estimated property obtained by spatial averaging of the stress, strain, or energy fields in the given domain [26]. The length in Figure 4 contains all three components no matter where on the composite structure this length is obtained. This length is the RVE (representative length element in this example).

Now consider for a moment if the sampling size must remain constant, and the exact same chain were then reduced in size, as in Figure 5. Now the sample size that was rejected in Figure 3 is acceptable as the RVE of the composite material. All elements of the composite material are present and the properties obtained (elongation) are representative of the composite material. If the reduction process is carried a step farther then more individual elements of the original composite fit within the constant sampling domain (Figure 6).

This is the approach used as proof in this work. The size of the beams used in the BBR is 12.7-mm x 6.35-mm x 127-mm. The main concern is regarding the largest aggregate sizes to smallest beam dimension ratio. For the 12.5-mm mixture this ratio is about 1 for the width of the beam and 2 for the thickness of the beam. This means that one aggregate could take up either of these dimensions entirely as seen in Figure 7.

This could be a problem if the desired property being evaluated were strength, but the property that the BBR measures is flexural creep modulus, which is averaged over the gage length of the composite material. This gage length is the length of the beam, not the width or the thickness. Therefore, in theory, it is valid to use the BBR to test mixture beams to obtain flexural creep modulus.

This work sets out to prove that the results from the BBR testing meet the RVE requirement by showing that the variance from the mixtures containing large (12.5-mm) aggregate particles is the same as the variances from the mixtures containing smaller (9.5-mm, 4.75-mm) aggregate particles. These three mixtures have the same volumetric parameters (volume fraction of components) as shown, both by physical, and visual measurements.

Figure 2: Composite Chain

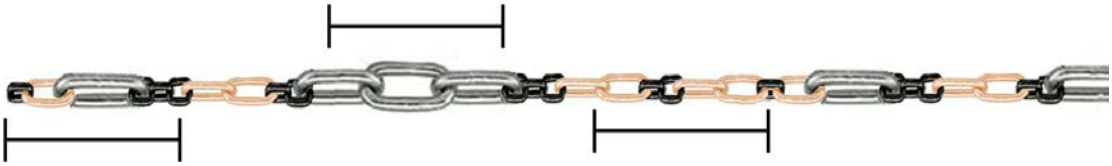

Figure 3: Composite Chain with Nonrepresentative Length

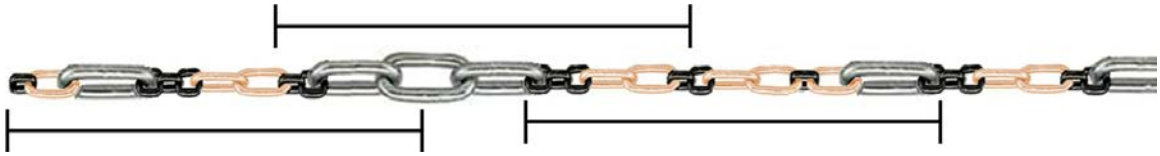

Figure 4: Composite Chain with RVE Length

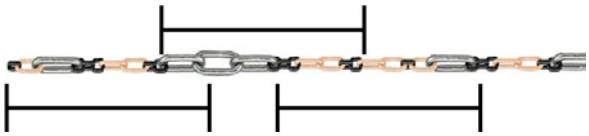

Figure 5: Composite Chain Reduced to 45% Original Size

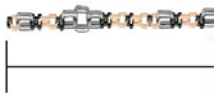

Figure 6: Composite Chain Further Reduced

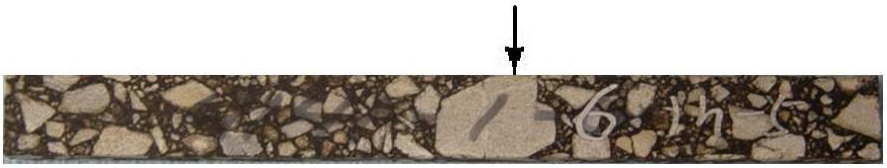

Figure 7: Example Beam with Large Aggregate Particle

MATERIALS AND PROCEDURES

The hypothesis of this work is that the large aggregate size (12.5-mm) in the mixture is not the cause of variability within the results of the BBR. This is proven by showing that the variability of the larger mixture is equivalent to the variability of the smaller NMAS mixture. This is done while maintaining equivalent volumetric parameters and gradation shape. If the variability is consistent then the hypothesis is supported, but if the variability is greatly affected then the hypothesis must be rejected.

In this research hot mix asphalt was used with a 12.5-mm NMAS mix as the standard mix. The performance grade (PG) 64-34 binder was selected for use because it has low temperature tolerance and is a relatively soft binder that will allow large movements when tested. The aggregate is of high quality quartz with very low absorption, this allows for easier modification of the mix design. Asphalt concrete was chosen as a good composite material to illustrate the hypothesis because it is a material with spatial disorder and no microstructural periodicity.

Volumetric Parameters

A voids analysis is very important while developing a gradation and mix design. It is important to understand the volumetric parameters of compacted asphalt concrete mixtures for both mix design and construction control. Many mix design methods

(including the Superpave mix design method, preferred by many department of transportations (DOTs) and government agencies) require the volumetric parameters to be within certain ranges. These parameters help standardize asphalt concrete mix designs and achieve certain desirable properties. The percent of voids in the mineral aggregate (VMA), is a measure of the space available in the aggregates for the addition of the asphalt cement. The voids filled with asphalt are called VFA and the total voids of the mix are called the VTM. Figure 8 depicts the components of the compacted asphalt mixture and the corresponding equations to calculate the volumetric parameters of the mixture.

As the NMAS of a mixture decreases the specific surface area of the mix increases, therefore, more asphalt is required to maintain a constant apparent film thickness (AFT) [27]. The film thickness is referred to as apparent because within the mixture a film thickness cannot truly be measured, it can only be estimated. Although the AFT can only be estimated it can be used to generalize comparisons between mixtures. For example an aggregate with a much smaller AFT will not have the same response as aggregate with a larger AFT as can be seen in Figure 9.

0.45 Chart Theory and Gradation

The 0.45 power chart is a common tool for Superpave gradation design. The horizontal scale is a 0.45 power function of the sieve size and the vertical scale is the percent of aggregate passing the corresponding sieve. The maximum density line on the 0.45 power chart represents a gradation of spheres of different sizes that create a mixture that has maximum theoretical density. This maximum density line is a straight line from

the origin to the NMAS of the mixtures. This line represents the gradation or particle size distribution that results in the highest level of packing, thus the highest bulk density. For example, Figure 10 shows the space between large aggregate represented by theoretical spheres. The space between these large spheres is then filled with the next largest sphere size, then the next size of spheres fill the resulting spaces; then, smaller spheres in the space around the those spheres; continuing into infinity, into theoretical maximum density, leaving no space or voids. Decreasing the NMAS would merely shift the maximum density line to the left of the chart but still result in the same level of packing as the larger NMAS max density line that is to the right.

Voids play an important role in asphalt mixture performance. There has to be enough voids in the mix to support the asphalt binder, which is the glue essentially, to keep the aggregate together. Too many voids and the mix will rut and too few voids and the mix will crack when placed in the field. An S shaped curve with respect to the maximum density line has been the preferred shape for Superpave gradation mix designs. This shape has shown good performance when used in conjunction with certain volumetric parameters.

The mixtures used in this work had NMAS of 12.5-mm, 9.5-mm, and 4.75-mm. The goal was to use the 12.5-mm aggregate gradation as the model and to scale the gradation curve to the other two respective NMAS sizes. The goal was not to merely eliminate the larger particles but have actual mixes with equivalent volumetric parameters and similar gradation shapes. The shape of each gradation curve was kept similar with respect to the maximum density line as seen in Figure 11. The gradations of the 12.5-mm, 9.5-mm, and 4.75-mm mixes used in this work are shown in Table 1.

In theory, similar shaped 0.45 gradations imply similar aggregate structure within the composite [28]. As the NMAS is reduced the amount of fines, and therefore aggregate surface area, increases. To match the VFA of the two developed mixes to the standard 12.5-mm mix, the binder content had to increase. This resulted in an increase in the VMA, but held the VFA constant. The goal was to keep the VFA and VTM constant, ensuring that proportionally the same amount of binder was present resulting in the same apparent film thickness on the particles. The gradation and binder content was adjusted several times through trial and error to accomplish similar gradation shape and volumetric parameters. A similar 0.45 gradation shape VTM, VMA, and VFA ensured that the mixes were essentially scaled equivalents of each other. Table 2 shows the volumetric properties of the three optimum asphalt concrete mixtures.

Bending Beam Rheometer

For this work the bending beam rheometer manufactured by Cannon Instrument Company was used. The BBR applies a constant load to the midpoint of a simply supported prismatic beam of, traditionally, asphalt binder. The dimensions of the beam used in the BBR are 12.7-mm width x 6.35-mm thickness x 127-mm length. The BBR measures the deflection at the midpoint due to a constant force applied at this midpoint. This BBR system consists of a loading frame within a temperature controlled bath and a computer controlled automated data acquisition unit. The bath uses ethylene glycol as a cooling medium. The Cannon BBR can maintain temperatures from ambient air to -36° ± 0.03° Celsius. To perform a test, a beam is placed in the bath and loaded with a constant force of 450 grams. As the beam creeps, the deflection at the midpoint is measured. This

equipment is capable of measuring at multiple times to determine the visco-elastic properties of the material. For this work the flexural creep modulus was recorded at 60 and 120 seconds. The flexural creep modulus controls the thermal stresses and is related to the damage that occurs to asphalt concrete termed, thermal fatigue cracking. Figure 12 shows a picture of the Cannon BBR and a diagram of the BBR simply supported beam mechanism within the temperature controlled bath.

Ho and Romero determined that at least twenty realizations for any one particular sample is required to accurately represent the population composite [18]. Therefore at least twenty beams were tested from each compacted mixture. The mixture “pucks” were of standard 150-mm diameter and were compacted using a gyratory compactor. The air voids within a puck are known to have a gradient distribution, where on the edges the voids may be slightly higher than in the middle of the puck. Therefore, testing twenty beams from each sample normalizes the variability that this gradient introduces. Using a lapidary saw, these pucks were cut into blocks, after which, the volumetric parameters were measured. These blocks were frozen to reduce excess heat developed when cutting into the small beams. A standard tile saw was used to cut the blocks into beams. For more detailed, step-by-step sample preparation, please refer to Romero and Ho’s work [18] - [20].

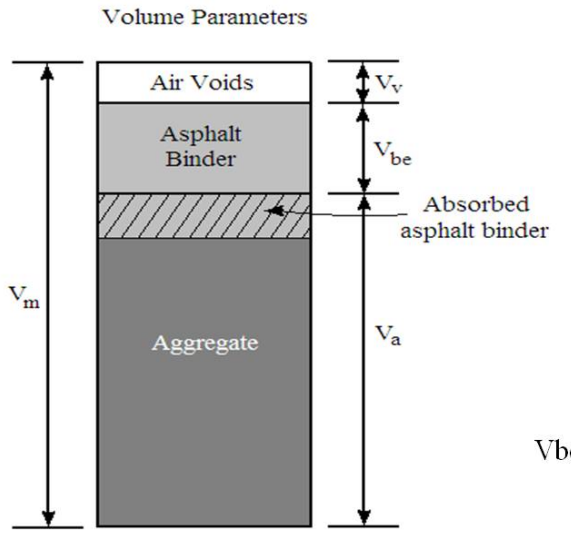

$$VTM = \frac{V_v}{V_m} 100$$

$$VMA = \frac{V_v + V_{be}}{V_m} 100$$

$$VFA = \frac{V_{be}}{V_{be} + V_v} 100$$

Vv = volume of air voids
Vbe = volume of effective asphalt binder
Vm = total volume of mixture

Figure 8: Components of Compacted Mixture with Volumetric Parameter Equations

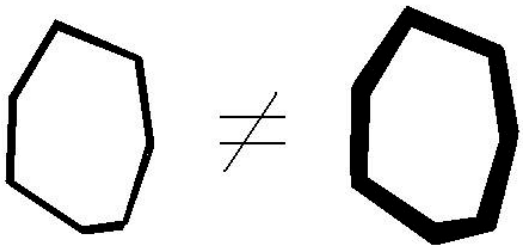

Figure 9: Unequal Film Thickness on Aggregate

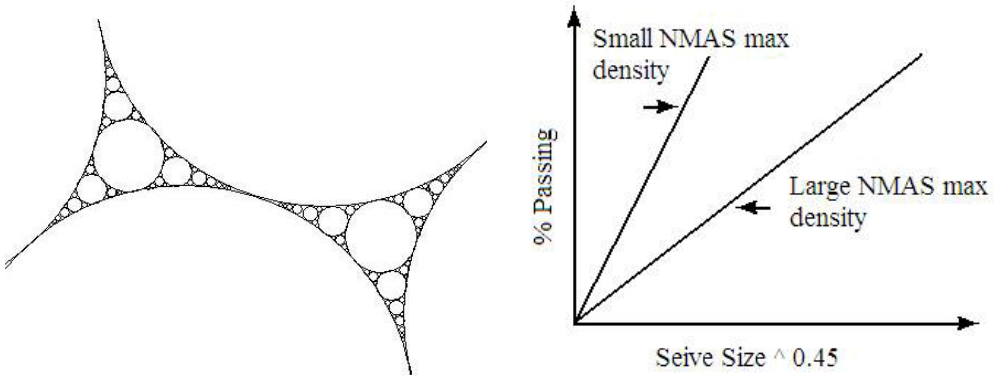

Figure 10: Schematic of Theoretical Maximum Density

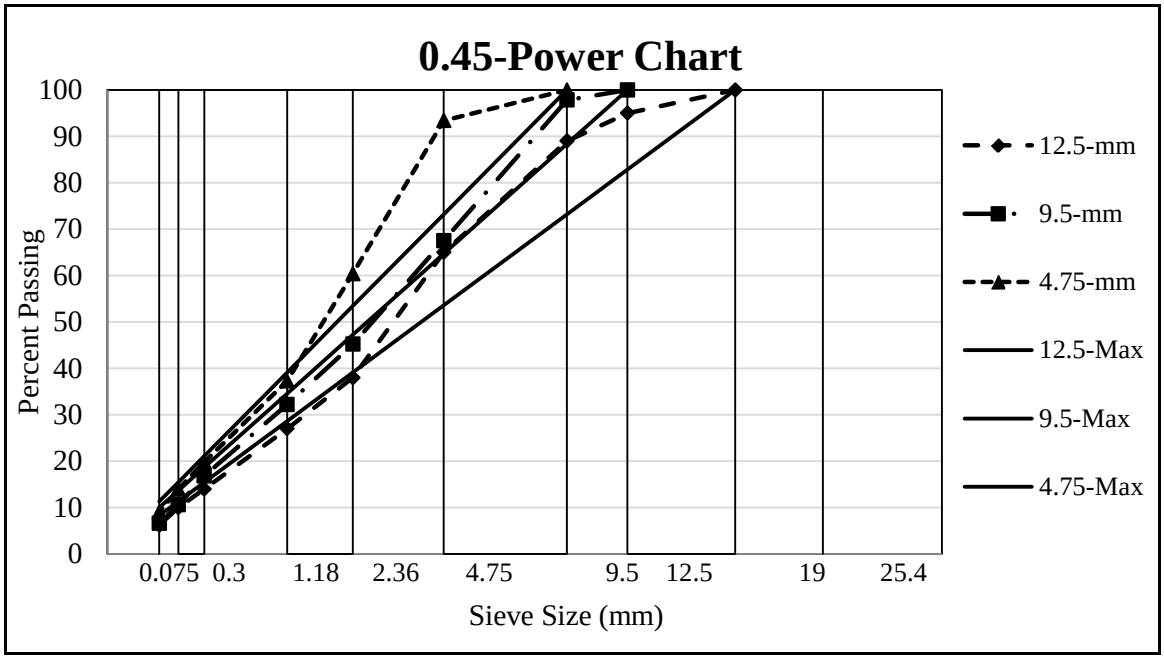

Figure 11: 0.45 Power Chart Depicting the Three Gradations Used for This Research

Table 1: Mixture Designs for the 12.5-mm, 9.5-mm, and 4.75-mm NMAS

Seive Size (mm)	Mixture Design		
	12.5-mm	9.5-mm	4.75-mm
	Percent Passing (%)		
19	100	100	100
12.5	95	100	100
9.5	89	97.8	100
4.75	65	67.5	84.9
2.36	38	45.2	60.4
1.18	27	32.2	37.3
0.3	14	16.8	19.8
0.149	10	10.6	14
0.075	6.2	6.6	9

Table 2: Volumetric Properties for the Three Mixtures

NMASS (mm)	Asphalt Content	VTM	VMA	VFA
4.75	6.5	4	17.19	79.05
9.5	6.2	4	16.70	78.44
12.5	6	4	16.38	78.03

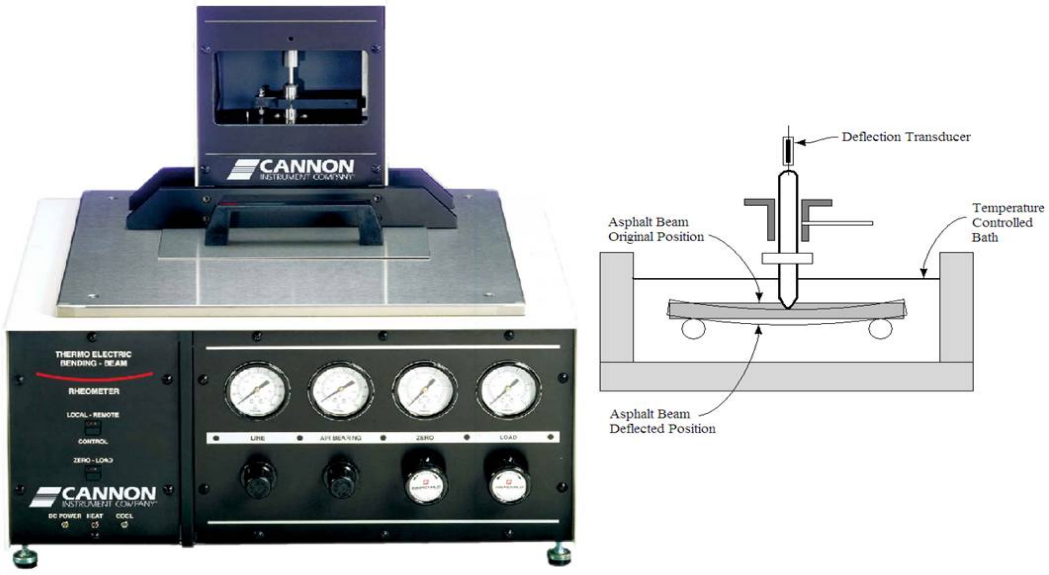

Figure 12: Bending Beam Rheometer with Simply Supported Beam Diagram

VERIFICATION OF NORMAL DISTRIBUTION

The hypothesis throughout this work is that all three different mixtures resulted in the same variability. Before a test on the homogeneity of variances could be performed, it was desirable to determine the distribution of the data sets. To accomplish this, graphical analysis along with tests based on empirical distribution function (EDF) statistics were applied to the BBR results [29].

We assume that the sample moduli of the asphalt mixtures are drawn from a normal distribution with density:

$$f(x) = \frac{1}{\sqrt{2\pi}\sigma} e^{-\frac{1}{2}\left[\frac{x-\mu}{\sigma}\right]^2} \quad (1)$$

where σ and μ are the estimated sample standard deviation and mean, and x is the value of the creep modulus measured. The CDF or cumulative distribution function for graphical analysis is the integral from -∞ to x of *f(x)*.

The ECDF or empirical cumulative distribution function is:

$$F_n(x) = \frac{\#(X_j \leq x)}{n}, -\infty < x < \infty \quad (2)$$

which is read, the number of X_j's less than or equal to x; and n is the number of realization in the sample set.

If we graph the CDF and the ECDF on the same graph we get a comparison of population and cumulative distribution functions for our sample data as in Figure 13 and Figure 14. These graphs can be used to determine if the ECDF is a "good fit" to the normal distribution or CDF. It may be difficult to scientifically determine that a distribution fits the normal cumulative curve by eye as in Figure 15. Therefore, tests based on EDF statistics were carried out on the data to be sure statistically that the data obtained from BBR testing is of a normal distribution.

The first two EDF statistics, D^+ and D^-, are, respectively, the largest vertical difference from $F_n(x)$ being larger than F(x), and the largest vertical difference from $F_n(x)$ being smaller than F(x) [29]. The quadratic statistics, a second and broad class of measures of discrepancy is the Cramér-von Mises family,

$$Q = n\int_{-\infty}^{\infty}\{F_n(x) - F(x)\psi(x)dF(x)\} \qquad (3)$$

where $\psi(x)$ is a function that give weights to the squared difference $\{F_n(x)\text{-}F(x)\}^2$. For $\psi(x)=1$ the statistic is the Cramér-von Mises statistic, called W^2, and for $\psi(x)=[\{F(x)\}\{(1\text{-}F(x)\}]^{-1}$ the statistic is the Anderson-Darling statistic, A^2. A modification of W^2 devised originally from the circle is the Watson statistic U^2 defined as

$$U^2 = n\int_{-\infty}^{\infty}\left\{F_n(x) - F(x) - \int_{-\infty}^{\infty}[F_n(x) - F(x)]dF(x)\right\}^2 dF(x) \qquad (4)$$

By using the Probability Integral Transformation (PIT), Z = F(X); when F(x) is the true distribution of X, the new random variable Z is uniformly distributed between 0 and 1; and has distribution function F*(z) = z, $0 \leq z \leq 1$ [29]. Samples X_1, .., X_n give values $Z_i = F(X_i)$, i = 1, …, n, and F*(z) is the EDF of the values Z_i. It can be shown that the vertical differences in the EDF diagrams for X and Z are equal, therefore EDF statistics calculated from the EDF of the Z_i compared with the uniform distribution will take equivalent values as if they were calculated from the EDF of the X_i, compared with F(x) [29]. This leads to the following formulas for calculating EDF statistics from the Z-values. The formulas require the Z – values to be arranged in ascending order, $Z_{(1)} < Z_{(2)} < ... < Z_{(n)}$. Then, with $\bar{Z} = \sum_i Z_i/n$,

$$D^+ = \max_i \left\{\frac{i}{n} - Z_i\right\};\ D^- = \max_i \left\{Z_i - \frac{(1-i)}{n}\right\} D = \max\ \ (D^+, D^-) \qquad (5)$$

$$V = D^+ + D^- \qquad (6)$$

$$W^2 = \sum_i \{Z_i - (2i-1)/(2n)\}^2 + \frac{1}{(12n)} \qquad (7)$$

$$U^2 = W^2 - n(\bar{Z} - 0.5)^2 \qquad (8)$$

$$A^2 = -n - (1/n)\sum_i [(2i-1)\ln(Z_i) + (2n+1-2i)\ln\{1-Z_i\}] \qquad (9)$$

These tests in order are the Kolmogorov-Smirnov D test, Kuiper V test, Cramer-von Mises W^2 test, Watson U^2 test and the Anderson-Darling A^2 test [29].

The general test of fit procedure can now be set out for EDF tests for Case 3, that is, for the null hypothesis H_0 : a random sample of n X-values comes from F(x;θ), where F(x;θ) is a continuous distribution and θ is a vector of parameters. For the normal distribution θ = (μ, σ^2), where for this case of unknown parameters (Case 3) in EDF tests for normal distribution both μ and σ are unknown, and are estimated by $\hat{\theta} = (\bar{X}, s^2)$ where $\bar{X}$ is the sample mean and $s^2 = \sum_i (X_i - \bar{X})^2/(n-1)$ [29].

Put the X_i in ascending order, $X_1 < X_2 < \ldots < X_n$.

Calculate w_i, for i = 1, …, n using $w_i = (X_i - \bar{X})/s$

Calculate $Z_i = \Phi(w_i)$, i = 1, …, n, where $\Phi(x)$ denotes the cumulative probability of a standard normal distribution N(0,1) to the value x.

Calculate the test statistics from equations 5, 6, 7, 8, and 9.

Using Table 3 the modified statistic is calculated. If the value of the modified statistic exceeds the appropriate percentage point at level α, H_0 is rejected with significance level α.

At significance level α = 0.01 all mixture creep modulus distributions modified EDF statistics fall below the tabulated values for the percentage points for a test for normality with μ and σ unknown. Therefore, it can be said, with a confidence level of 99%, that all sample sets from this work are of normal distribution.

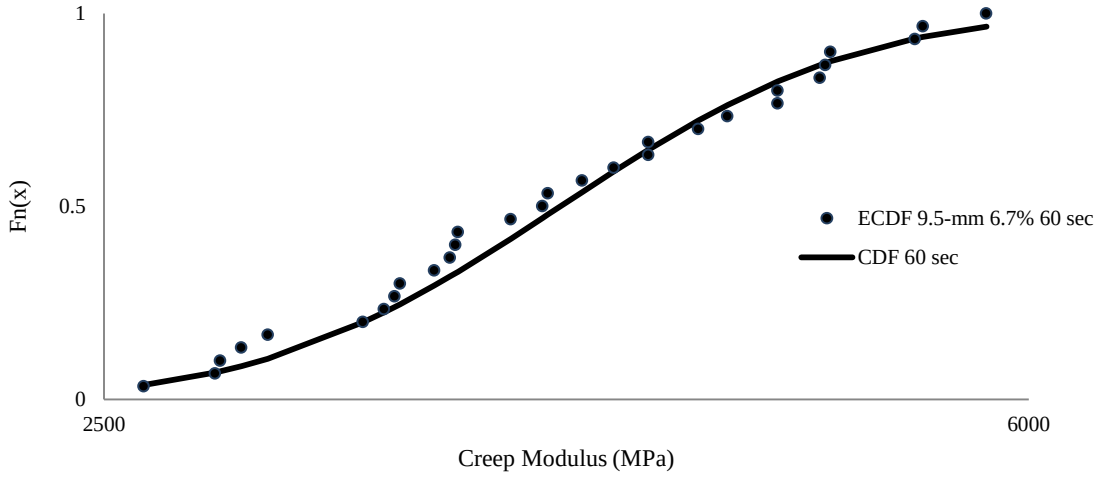

Figure 13: Comparison of Population and Empirical Cumulative Distribution Functions for 9.5-mm mix 6.7% AC at 60 sec

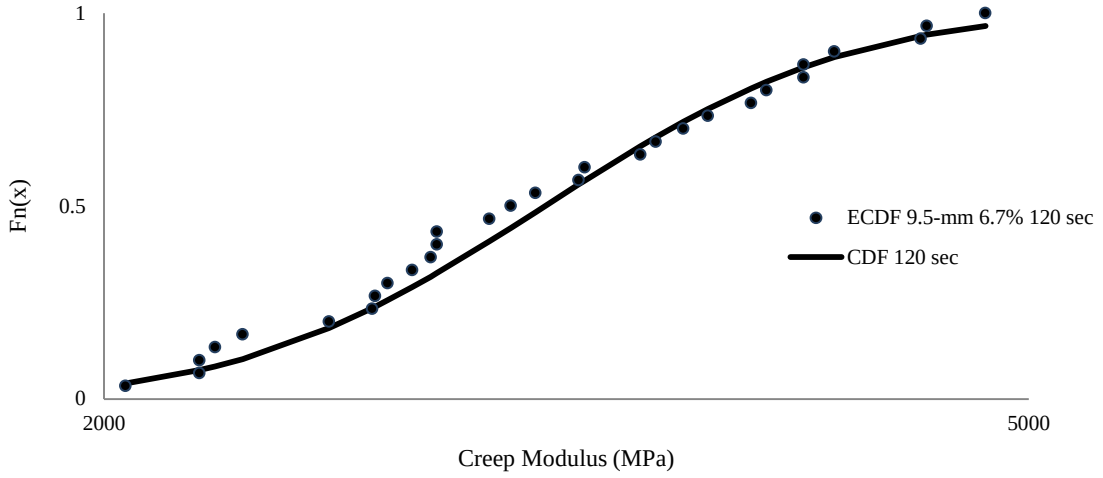

Figure 14: Comparison of Population and Empirical Cumulative Distribution Functions for 9.5-mm mix 6.7% AC at 120 sec

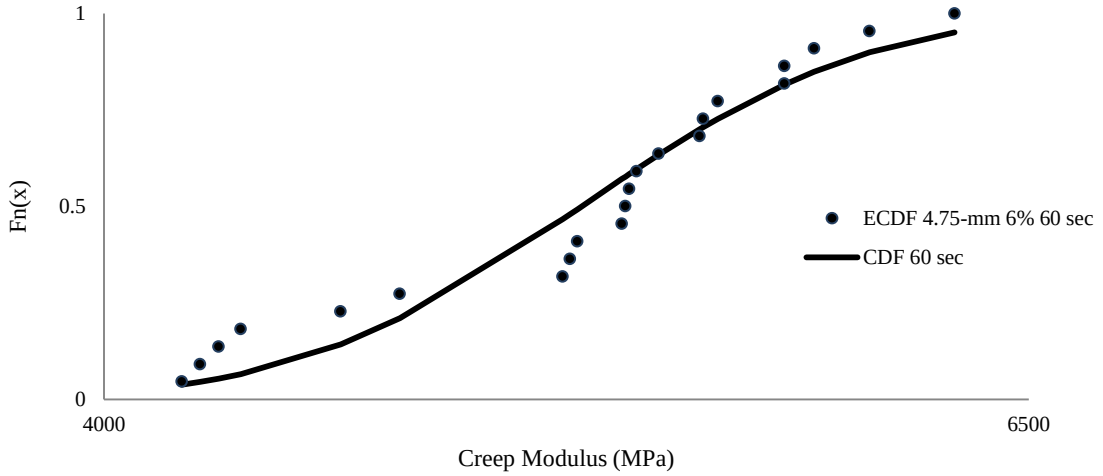

Figure 15: Comparison of Population and Empirical Cumulative Distribution Functions for 4.75-mm mix 6% AC at 60 sec

Table 3: Modifications and Percentage Points for a Test for Normality with μ and σ Unknown

Statistic	Modified Statistic	Significance Level α					
		.15	.10	.05	.025	.01	.005
D	$D\left(\sqrt{n} - 0.01 + 0.85/\sqrt{n}\right)$	0.775	0.819	0.895	0.995	1.035	
V	$V\left(\sqrt{n} + 0.05 + 0.82/\sqrt{n}\right)$	1.320	1.386	1.489	1.585	1.693	
W2	$W^2(1.0 + 0.5/n)$	.091	.104	.126	.148	.179	.201
U2	$U^2(1.0 + 0.5/n)$	.085	.096	.117	.136	.164	.183
A2	$A^2(1.0 + 0.75/n + 2.25/n^2)$	.561	.631	.752	.873	1.035	1.159

Note: Adapted from Table 4.7 of D'Agostino and Stevens (1986)

HOMOSCEDASTICITY OF VARIANCES

Three NMAS groups were developed for this research to explore possible sources of variability with respect to aggregate size. If the variances of the three NMAS are equal then we know that the size of the aggregate does not affect the variability of the data and we can conclude that a beam made with the 12.5-mm NMAS mixture is, in fact, a representative volume element (RVE) of the overall mixture. In other words, the BBR results are valid. The most robust method to evaluate the homoscedasticity of variances is the Levene test. But, if there is strong evidence that the data do, in fact, come from a normal distribution, Bartlett's test has better performance [30]. Because the tests based on EDF statistics confirmed that all our data sets are of normal distribution, the Bartlett's test was selected to test for the homogeneity of variances. Bartlett's test is defined as:

Hypothesis: $\sigma_a^2 = \sigma_b^2 = \cdots = \sigma_k^2$

$\sigma_a^2, \sigma_b^2,$ and σ_c^2 signify the variances of the 3 NMAS groups.

Test guide:

$$T = \frac{(N-k)\ln\left(s_p^2\right) - \sum_{i=1}^{k}(N_i - 1)\ln(s_i^2)}{1 + \left(\frac{1}{3(k-1)}\right)\sum_{i=1}^{k}\left(\frac{1}{N_i - 1}\right) - \frac{1}{N-k}} \tag{10}$$

where N is the total sample size, s_i^2 is the variance of the *i*th group, N_i is the sample size of the *i*th group, k is the number of groups, and s_p^2 is the pooled variance. The pooled variance is a weighted average of the group variances and is defined as:

$$s_p^2 = \frac{\sum_{i=1}^{k}(N_i-1)s_i^2}{N-k} \tag{11}$$

With significance level α the variances are judged to be unequal if

$$T > X^2_{(1-\alpha,k-1)} \tag{12}$$

where $X^2_{(1-\alpha,k-1)}$ is the upper critical value of the chi-square distribution, with $k-1$ degrees of freedom. If $T < X^2_{(1-\alpha,k-1)}$ we fail to reject the null hypothesis and the mixtures have equal variances. We concentrated first on the optimum asphalt content for the three different NMAS. For the optimum asphalt contents there were twenty-five of the 12.5-mm NMAS, twenty-seven of the 9.5-mm NMAS, and twenty nine of the 4.75-mm NMAS samples used for the Bartlett's test, for a total of eighty-one samples. Applying Equations 10, 11, and 12 to our sample groups, we test the hypothesis that our sample groups have equal variances.

Table 4 depicts the results of the Bartlett's test on our equal variance hypothesis. The Bartlett's test shows that the variances of these three groups are in fact identical.

In statistics a Type I error is to reject the null hypothesis when, in fact, the null hypothesis is true. A type II error is to accept the null hypothesis when, in fact, the null hypothesis is false. Ho and Romero discuss how De Veaux et al. state that the only way

to reduce both Type I and II error is to increase the sample size [19]. Ho and Romero concluded that the minimum number of replicates for any given sample is fifteen, to bring the coefficient of variation to stability. It is summarized that at fifteen samples the probability of making a Type I or Type II error is minimized. Because, for this work, at least twenty-two replicates were tested for each sample, it is shown that the chance a Type I or II error was made is minimal.

Through Bartlett's test the three sample groups at optimum asphalt content fail to reject H_0. This supports our hypothesis that even with an NMAS of 12.5-mm the small beams of dimensions 12.7-mm x 6.35-mm x 127-mm do not introduce excess variability. Since the mixture with the NMAS of 12.5-mm has aggregate that is larger than the smaller dimensions of the beam it can be extended for the NMAS sizes evaluated that when measuring the global properties of the mixture such as the stress or strain; the aggregate size does not have an effect on the variance of the sample group. Because the variability of the sample groups remains constant, the test is not adversely affected by the large aggregate. It can be extended further that the smaller NMAS; with an increased amount of aggregate in the small size beams, does not increase the variability either.

Six other groups were developed by mixing binder sweeps of the optimum asphalt content for each mixture. H_0 was tested using Bartlett's test with k=18. This included the three optimum mixtures with asphalt content ±0.5% with each of those nine mixtures having creep modulus at 60 seconds and 120 seconds. This resulted in eighteen sample groups. For k-1 = 17 and $\alpha = 0.05$; $X^2_{(1-\alpha,k-1)} = 27.587$ and T = 27.277. $T < X^2_{(1-\alpha,k-1)}$. Bartlett's test fails to reject H_0, and all eighteen sample groups have equal variances.

Table 4: Bartlett's Test

H0:	$\sigma^2_{12.5NMAS} = \sigma^2_{9.5NMAS} = \sigma^2_{4.75NMAS}$							
HA:	The three samples variances are heterogeneous							
Group	12.5 NMAS Creep Modulus at 60 sec. (GPa)		9.5 NMAS Creep Modulus at 60 sec. (GPa)		4.75 NMAS Creep Modulus at 60 sec. (GPa)		k=3	
	2.94	4.38	5.08	7.1	4.64	6.35		
	3.17	4.43	5.12	7.11	4.79	6.47		
	3.27	4.57	5.28	7.16	5.03	6.55		
	3.82	4.76	5.7	7.18	5.2	6.62		
	3.94	4.78	5.77	7.2	5.22	6.67		
	4.03	4.97	6.08	7.44	5.24	6.72		
	4.04	4.97	6.27	7.56	5.29	6.77		
	4.06	4.99	6.61	7.73	5.43	6.81		
	4.09	5.23	6.73	7.75	5.56	6.84		
	4.1	5.31	6.74	8.31	5.6	6.88		
	4.13	5.79	6.77	8.57	5.66	6.9		
	4.16	5.81	6.82	8.78	5.76	6.98		
	4.22		6.85	8.83	6.07	7.06		
			7.1		6.31	7.64		
					6.31			
N_i	25		27		29		$N = \sum N_i$	81
s_i^2	0.5392		1.0586		0.6269			
$s_p^2 = \frac{\sum_{i=1}^{k}(N_i - 1)\, s_i^2}{N - k}$							0.7438	
$B = (N-k)\ln(s_p^2) - \sum_{i=1}^{k}(N_i - 1)\ln(s_i^2)$							3.3346	
$C = 1 + \left(\frac{1}{3(k-1)}\right)\sum_{i=1}^{k}\left(\frac{1}{N_i - 1}\right) - \frac{1}{N-k}$							1.0258	
$T = \frac{B}{C}$			3.2508		$X^2_{(\alpha=0.05,2)}$		5.991	

Conclusion: T $< X^2_{(1-\alpha,k-1)}$, we fail to reject H0

SCALED MIXTURES

Most of the literature can agree that the aggregate or fines passing the 0.075-mm sieve is filler and does not interact directly with the larger aggregate. Although this filler does affect some properties of the mix, for the purposes of this visual analysis, it will not be considered to affect the skeleton of the mixture. This mineral filler has an upper limit requirement of all passing the 0.6-mm sieve. Consequently, any aggregate larger than the 0.6-mm sieve could be contributing to the structural integrity of the asphalt mixture. Greene theorized that the dominant aggregate size range (DSAR) is the interactive range of particle sizes that form the primary structural network of aggregates, and for the 12.5-mm mix only particle sizes greater than 1.18-mm can be considered coarse enough to provide the particle interlock necessary to resist permanent deformation [31]-[32]. For the purposes of this visual analysis we will solely be concerned with the aggregate sizes that directly contribute to the skeleton of the mixture. This includes all aggregate larger than the 0.6-1.18 mm range. Conveniently, this range of aggregate size is the smallest range that the eye can clearly see in a scanned image.

At a midpoint in the beam cutting process, each block of the optimum mixtures was scanned. The scanned images of the optimum asphalt content mixtures for the 12.5-mm, 9.5-mm, and 4.25-mm were scaled to 50%, 66%, and 100% original size, respectively; this can be seen in Figure 16. This scaling is based on the US customary measurements where the 4.75-mm = 0.25 inch NMAS, 9.5-mm = 0.375 inch NMAS, and

12.5-mm = 0.5 inch NMAS. The 0.5 inch NMAS is two times the size of the 0.25 inch NMAS and the 0.375 inch NMAS is one and one-half times the size of the 0.25 inch mix. Using the 0.25 inch mix at 100% to scale from, we scale $\frac{0.25\ inch\ mix}{0.50\ inch\ mix} = {}^{1}/_{2}$ x 100% = 50% and $\frac{0.25\ inch\ mix}{0.375\ inch\ mix} = {}^{1}/_{1.5}$ x 100% = 66%. An alternative scaling scheme could be to increase the 4.75-mm mixture x 200% and the 9.5-mm mixture x 150% and keep the 12.5-mm mixture x 100% but this scheme resulted in issues with the image clarity. The resolution of the scanned images was not high enough to support this kind of magnification.

Figure 18 depicts how area 5 from each mixture was then cropped and magnified to 300%. This was done for all thirteen areas. Any aggregate visually identifiable within a given area was tallied. If the number of aggregate tallied within each area of the three mixtures is roughly the same we can further confirm that the two smaller NMAS mixtures are, in fact, scaled equivalents of the 12.5-mm NMAS mix because the solids in the volume fraction images are roughly the same. The tallied aggregate were, in fact, statistically equivalent. Table 4 shows the summary of the scaled mixtures analysis.

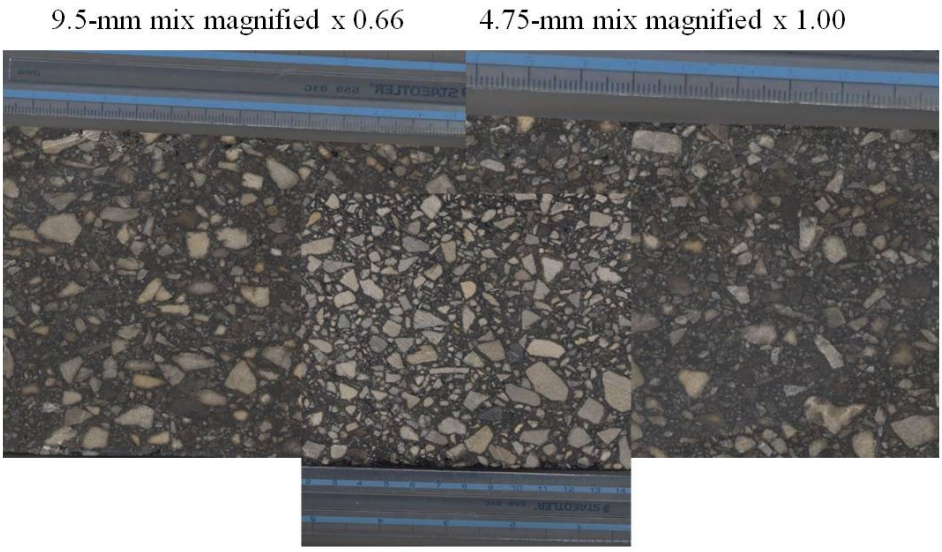

Figure 16: Optimum Mixtures Scanned and Scaled

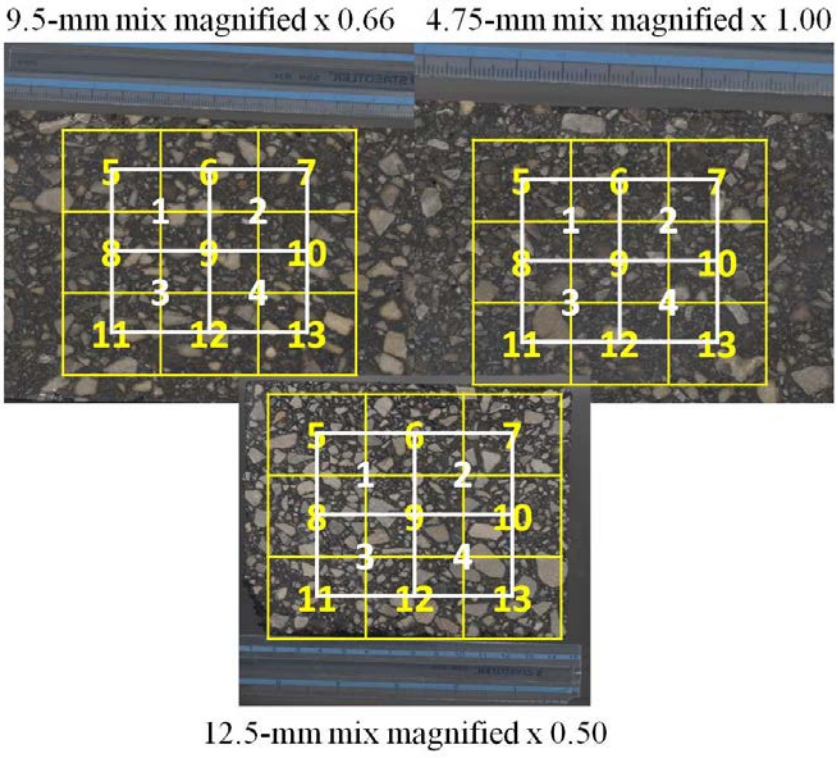

Figure 17: Scanned and Scaled Mixtures Divided into Thirteen Sections

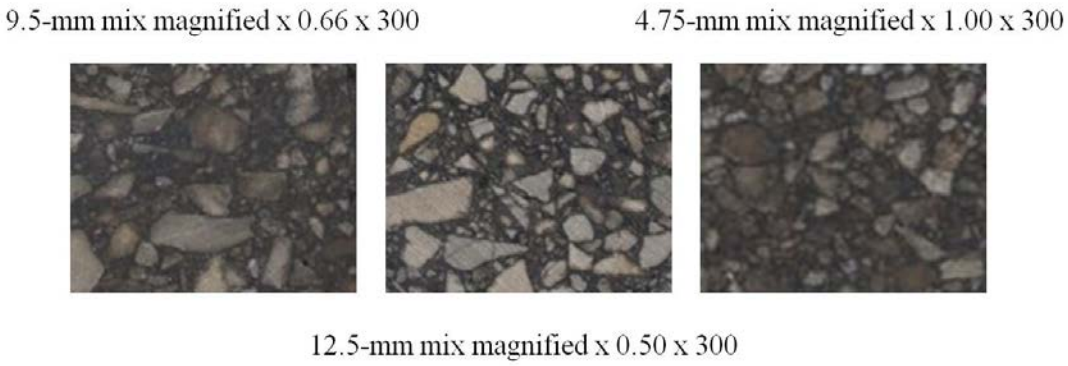

Figure 18: Area 5 of Each Mixture Magnified to 300% of Scaled Image

Table 5: Summary of Analysis of Scaled Mixtures

Analysis of Scaled Mixtures			
NMAS Area	12.5 –mm	9.5-mm	4.25-mm
	(Number of Tallied Aggregate)		
1	295	285	304
2	297	292	283
3	325	321	265
4	283	250	310
5	297	267	271
6	286	253	285
7	290	330	295
8	318	350	276
9	297	300	340
10	296	263	269
11	333	267	287
12	271	266	296
13	251	267	310
Total	3839	3711	3791
Average	295	285	292
Standard Deviation	22	31	21
Median	296	267	287
Range	251-333	250-350	265-340

SUMMARY AND CONCLUSIONS

The importance of keeping costs down while maintaining technicality is a paramount key in developing any test, standard, or specification. Most DOTs, as well as research laboratories, utilize the BBR and are very familiar with the operation of the BBR. This machine can produced same-day results pertaining to a mixture being put into use. That is to say, a test could be conducted on the same day as a pavement is being laid and thus give accurate, affordable, simple, repeatable, essential information about the mixture being laid. This essential information could raise awareness about inconsistencies of mixtures from day to day during the road construction, or show deviations from a mixture specification established prior to construction. Utilizing the BBR could potentially achieve this.

In this work it has been shown that three mixtures of descending NMAS can be created to evaluate if the size of the large particles affect the variability of the results obtained from BBR measurements. The results show that in utilizing the BBR to test asphalt concrete mixtures, NMAS as large as 12.5-mm do not introduce any excess variability than a smaller NMAS of 9.5-mm or 4.75-mm at the sample dimensions recommended for use in the BBR (12.7 mm x 6.35 mm x 127-mm). Therefore, the 12.5-mm NMAS can be used with confidence in the BBR at the specified beam size. One puck of standard dimensions of 150-mm diameter and 100-mm height can yield close to fourty

samples within dimensional tolerances. This can be achieved with a simple lapidary saw, freezer, and tile saw [18], [20].

Summary of Observations

- The sample groups in this work were found to be of normal distributions with equal variances.
- Within a constant area the 4.75-mm mixture was found to have twice the amount of solids as the 12.5-mm mixture and the 9.5-mm mixture was found to have one and a half times as many solids as the 12.5-mm mixture.
- Large aggregate taking up the entire width and/or thickness dimensions of the beams do not create outliers within the data sets because the gage length is the *length* of the beam when determining the flexural creep modulus.
- It is simple to obtain flexural creep modulus of small asphalt mixture beams using the BBR.

Conclusions

Based on the work done as part of this thesis, it is concluded that using the BBR to test mixtures could be a viable answer to getting fast, inexpensive, and crucial information about a mixture for quality control as well as incorporating parameters for cold temperature properties.

SUGGESTIONS FOR FUTURE WORK

- Determine if the strength of asphalt concrete mixtures at low temperatures can be accurately determined using a similar approach as carried out in this work.
- Investigate if asphalt mixtures having larger NMAS than 12.5 can be tested using a similar approach as outlined in this thesis.

REFERENCES

[1] M. Marasteanu, A. Zofka, M. Turos, X. Li, R. Valasques, W. Buttlar, G. Paulino, A. Braham, E. Dave, O. Ojo, H. Bahia, C. Williams, J. Bausano, Al Gallistel, and J. McGraw. "Investigation of Low Temperature Cracking in Asphalt Pavements." National Pooled Fund Study 776. Report MN/ RC 2007-43 Minnesota Department of Transportation, October 2007.

[2] American Association of State Highway and Transportation Officials. "Standard Test Method for Indirect Tensile (IDT) Strength of Bituminous Mixtures." Standard Specifications for Transportation Materials and Methods of Sampling and Testing T 322. AASHTO 29th edition, 2009.

[3] R. Roque, D.R. Hiltunen, and W.G. Buttlar. "Thermal Cracking Performance and Design of Mixtures Using Superpave." *Journal of the Association of Asphalt Paving Technologist,* vol. 64, pp. 718-735, 1995.

[4] R. Lytton, J. Uzan, E. G. Fernando, R. Roque, D. Hiltunen, and S. Stoffels. "Development and Validation of Performance Prediction Models and Specifications for Asphalt Binders and Paving Mixes." *SHRP Report:* SHRP-A-357, Washington, D.C., 1993.

[5] W.G. Buttlar, and R. Roque. "Determination and Evaluation of the Strategic Highway Research Program Measurement and Analysis System for Indirect Tensile Testing at Low Temperature." *Journal of Transportation Research Board, Transportation Research Record of the National Academies*, No. 1454, Washington D.C., pp. 163-171, 1994.

[6] R. Roque, and D.R. Hiltunen. "Use of Canadian SHRP Test Sections to Evaluate the SHRP Indirect Tensile Creep and Failure Test for Control of Thermal Cracking," in *Proc. of the Canadian Technical Asphalt Association*, vol. XXXIX, 1994, pp. 441-464.

[7] American Association of State Highway and Transportation Officials. "Standard Method for Testing Asphalt Mixtures Using the Thermal Stress Restrained Specimen Test (TSRST)." U.S. Provisional Standard TP10, 2000.

[8] D. Jung, and T.S. Vinson. “Low Temperature Resistance of Asphalt Concrete Mixtures.” *Asphalt Paving Technology, Journal of the Association of Asphalt Paving Technologists*, vol. 62, pp. 54-92, 1993.

[9] C. L. Monismith, G.A. Secor, and K.E. Secor. “Temperature Induced Stresses and Deformations in Asphalt Concrete.” *Journal of the Association of Asphalt Paving Technologist*, vol. 34, pp. 248-285, 1965.

[10] M.P. Wagoner, W.G. Buttlar, and G.H. Paulino. “Disk-Shaped Compact Tension Test for Asphalt Concrete Fracture.” *Society for Experimental Mechanics*, vol. 45, No. 3, pp. 270-277, 2005.

[11] American Society of Testing and Materials. “Standard Test Method for Determining Fracture Energy of Asphalt Aggregate Mixtures Using the Disk-Shaped Compacted Tension Geometry.” U.S. ASTM Standard D731307-07.

[12] S. Charmot, and P. Romero. “Fracture Energy Evaluation of Cold In-Place Recycling Mixtures” in *Advanced Testing and Characterization of Bituminous Material*, Two Volume Set (ATCBM09), Loizos, Parti, Scarpas, and Al-Qadi, Ed. New Mexico: CRC Press, May 2009, ISBN 978-0-415-55854-9, pp. 1123-1130.

[13] S. Charmot, and P. Romero. “Assessment of Fracture Parameters to Predict Field Cracking Performance of Cold In-Place Recycling Mixtures.” *Journal of the Transportation Research Board*, No 2155 Paper 10-1773, pp. 34-43, 2010.

[14] A. Zofka, M.O. Marasteanu, Xinjun Li, T.R. Clyne, and J. McGraw. “Simple Method to Obtain Asphalt Binders Low Temperature Properties from Asphalt Mixtures Properties.” *Journal of the Association of Asphalt Paving Technologists*, vol. 74, pp. 255-282, 2005.

[15] A. Zofka. “Investigation of Asphalt Concrete Creep Behavior Using 3-Point Bending Test” presented at University of Minnesota, Minneapolis, Jul. 2007.

[16] A. Zofka, M. Marasteanu, and M. Turos. “Investigation of Asphalt Mixture Creep Compliance at Low Temperatures.” *Journal of Road Materials and Pavement Design*, vol. 9, pp. 269-286, 2008.

[17] A. Zofka, M. Marasteanu, and M. Turos. “Determination of Asphalt Mixture Creep Compliance at Low Temperatures Using Thin Beam Specimens.” *Journal of the Transportation Research Board*, No. 2057, pp. 134-139, 2008.

[18] C.H. Ho, and P. Romero. “Using Asphalt Mixture Beams in the Bending Beam Rheometer.” *International Journal of Road Materials and Pavement Design*, Lavoisier ISSN 1468-0629, vol. 12 – No2/2011, pp. 293-314, 2011.

[19] C.H. Ho, and P. Romero. “Asphalt Mixture Beams Used in Bending Beam Rheometer for Quality Control” *Journal of the Transportation Research Board Washington DC*, Issue 2268/2012, pp. 92-97, 2012.

[20] P. Romero, C.H. Ho, and K. VanFrank. “Development of Methods to Control Cold Temperature and Fatigue Cracking of Asphalt Mixtures.” *Utah Department of Transportation Research Division*, Report No. UT-10.08, May 2011.

[21] R. Velásquez, M. Labuz, M. Marasteanu, and M. Turos. “Chapter 31. Effect of Beam Size on the Creep Stiffness of Asphalt Mixtures at Low Temperatures.” *Advanced Testing and Characterization of Bituminous Materials*, Two Volume Set (ATCBM09). Loizos, Parti, Scrapas, and Al-Qadi, Ed. New Mexico: CRC Press, May 2009, ISBN 978-0-415-55854-9, pp. 313-322.

[22] P. Romero, and E. Masad. “Identifying the Relationship Between the Representative Volume Element and Mechanical Properties of Asphalt Concrete.” *Journal of Materials in Civil Engineering*, vol. 12, No. 1. American Society of Civil Engineers, pp. 77-84, 2001.

[23] X. Du, and M. Ostoja-Starzewski. “On the Scaling from Statistical to Representative Volume Element in Thermoelasticity of Random Materials.” *Networks and Heterogeneous Media*, vol. 1, No. 2, pp. 259-274, Jun. 2006.

[24] M. Ostoja-Starzewsky. “Materials Spatial Randomness: From Statistical to Representative Volume Element.” *Probabilistic Engineering Mechanics*, vol. 21, No. 2, ISSN 0266-8920, pp. 112-132, 2006.

[25] Z. Hashin, “A Variational Approach to the Theory of Elastic Behavior of Multiphase Materials.” *Journal of the Mechanics and Physics of Solids*, vol. 11, Issue 2, pp. 127-140, Apr. 1963.

[26] T. Kanit, S. Forest, I. Galliet, V. Mounoury, and D. Jeulin. “Determination of the Size of the Representative Volume Element for Random Composites: Statistical and Numerical Approach.” *International Journal of Solids and Structures*, vol. 40, pp 3647-3679, Jun.-Jul. 2003.

[27] Donald W. Christensen Jr, Roman F. Bonaquist. “Volumetric Requierments for Superpave Mix Design.” *Transportation Research Board, Washington, D.C.,* NCHRP Report 567, 2006. www.onlinepubs.trb.org/onlinepubs/nchrp/nchrp_rpt_567.pdf, [2006].

[28] J.F. Goode and L.A. Lufsey. “A New Graphical Chart for Evaluating Aggregate Gradations,” in *Proc. of the Association of Asphalt Paving Technologist*, vol. 31, Jan. 29-31, 1962, pp 176-207.

[29] Ralph B. D’Agostino, and Michael A. Stephens. *Goodness-of-Fit Techniques (Statistics: a Series of Textbooks and Monographs,* vol. 68. New York: Dekker, 1986.

[30] J.H. Zar. *Biostatistical Analysis. Fourth edition*. New Jersey: Prentice Hall, 1999.

[31] J. Greene, S. Kim, and B. Choubane. “Accelerated Pavement Testing of a HMA Gradation-Based Evaluation Method State of Florida Department of Transportation” *State Materials Office*, FL/DOT/SMO/10-539, Dec. 2010.

[32] S. Kim, R. Roque, A. Guarin, and B. Birgisson. “Identification and Assessment of the Dominant Aggregate Size Range (DASR) of Asphalt Mixture.” *Journal of the Association of Asphalt Paving Technologists*, vol. 75, pp 789-814, 2006.